

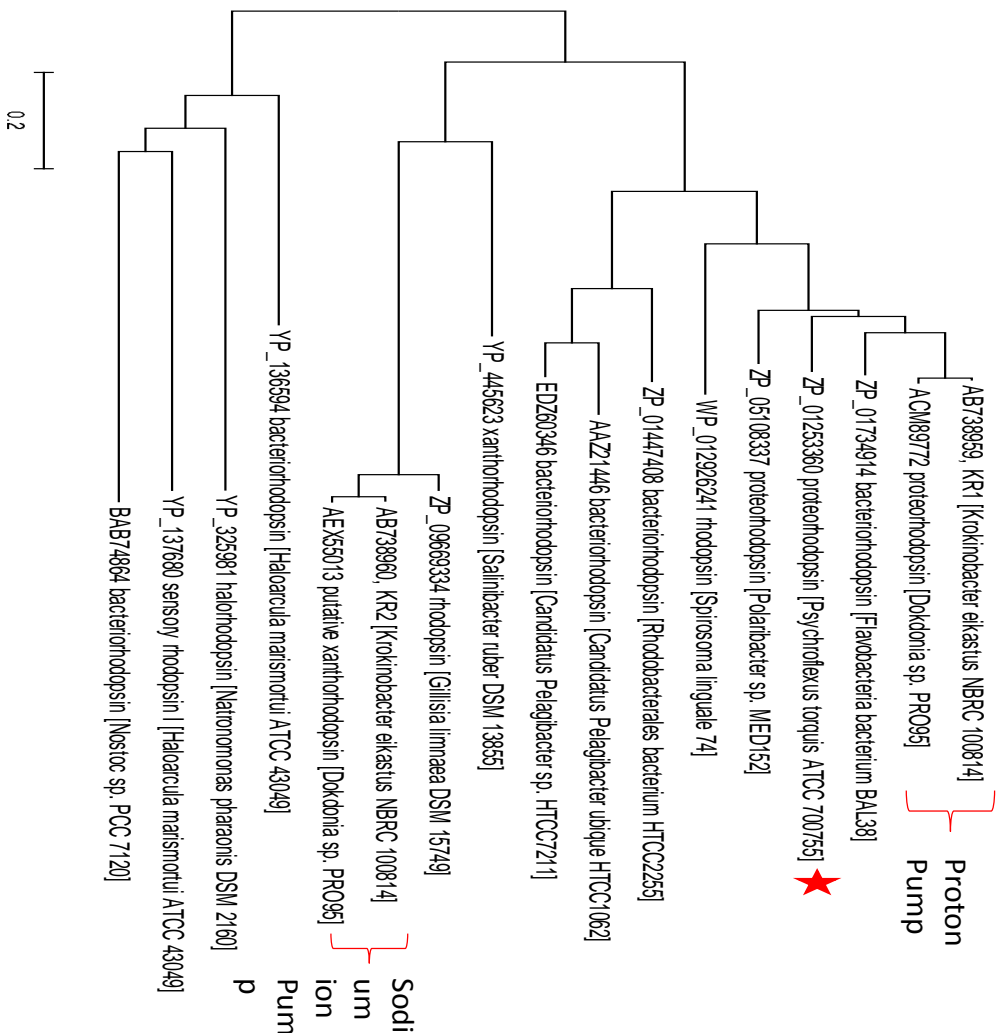
Proteomic insight into functional changes of proteorhodopsin-containing bacterial species *Psychroflexus torquis* under different illumination and salinity levels

Shi Feng¹, Shane M. Powell¹, Richard Wilson² & John P. Bowman¹

1. Food Safety Centre, Tasmanian Institute of Agriculture, University of Tasmania, Sandy Bay, Hobart, Tasmania 7005, Australia.
2. Central Science Laboratory, University of Tasmania, Sandy Bay, Hobart, Tasmania 7005, Australia.

TABLE OF CONTENTS

Supplemental Figure S1. Phylogenetic tree of microbial rhodopsins' amino acid sequences, and signature sequence comparison of proton pumping and sodium ion pumping rhodopsin	Page S-2
Supplemental Figure S2. Growth of <i>P. torquis</i> in modified marine broth.	Page S-3
Supplemental Figure S3. Spectral counts of <i>P. torquis</i> proteins.	Page S-4
Supplemental Figure S4. Volcano plot of proteins from high light condition compare to low light condition.	Page S-5
Supplemental Figure S5 Proteomic response of electron transport chain proteins under different salinities.	Page S-6
Supplemental Figure S6. Diagram of central metabolic pathway change under different salinity level.	Page S-7
Supplemental Figure S7. Gliding motility of <i>P. torquis</i> under different salinity and illumination level.	Page S-8
Supplemental Table S1. Spectral count and number of protein identified by LC-MS/MS from each sample.	Page S-9



B

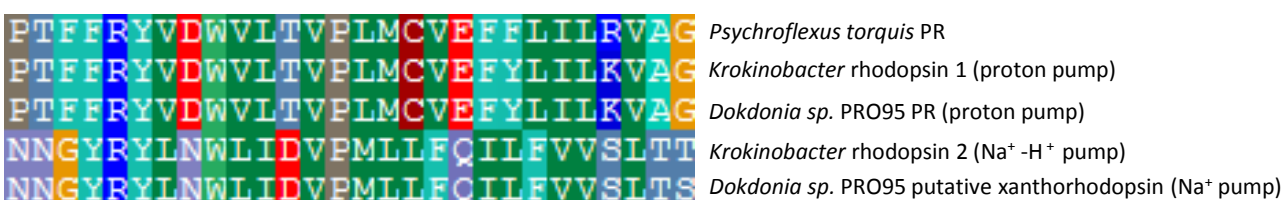


Figure. S1. (A) Phylogenetic tree constructed based on rhodopsin protein sequences using Neighbor-joining method. Proteorhodopsin harbored by *P. torquis* is closest to known proton pumping rhodopsins. (B) Amino-acid sequence comparison of the C-helix in proton pumping and sodium ion pumping rhodopsins.

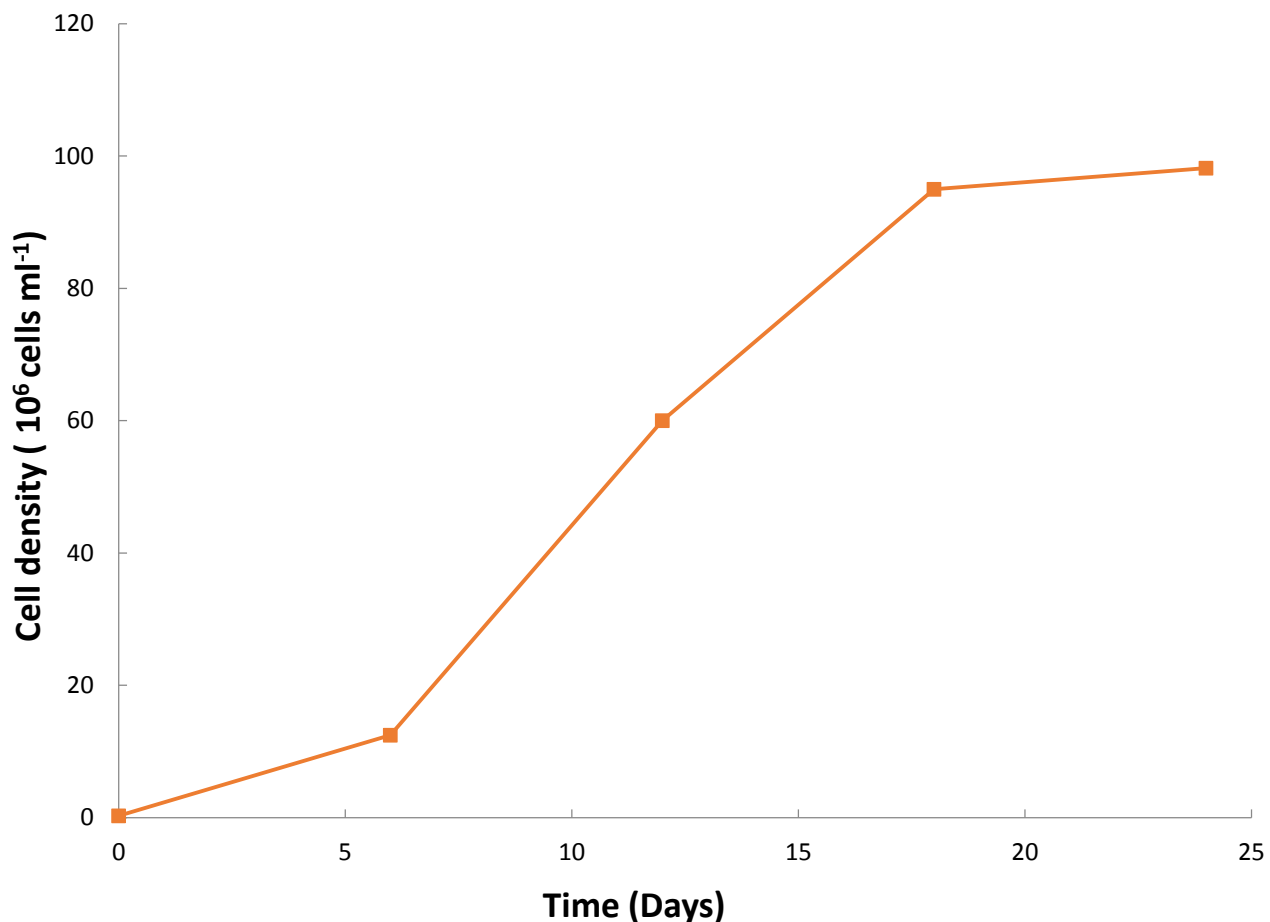


Figure. S2. Growth of *P. torquis* in marine broth. Bacterial cell densities were determined in triplicates by direct count under light microscope.

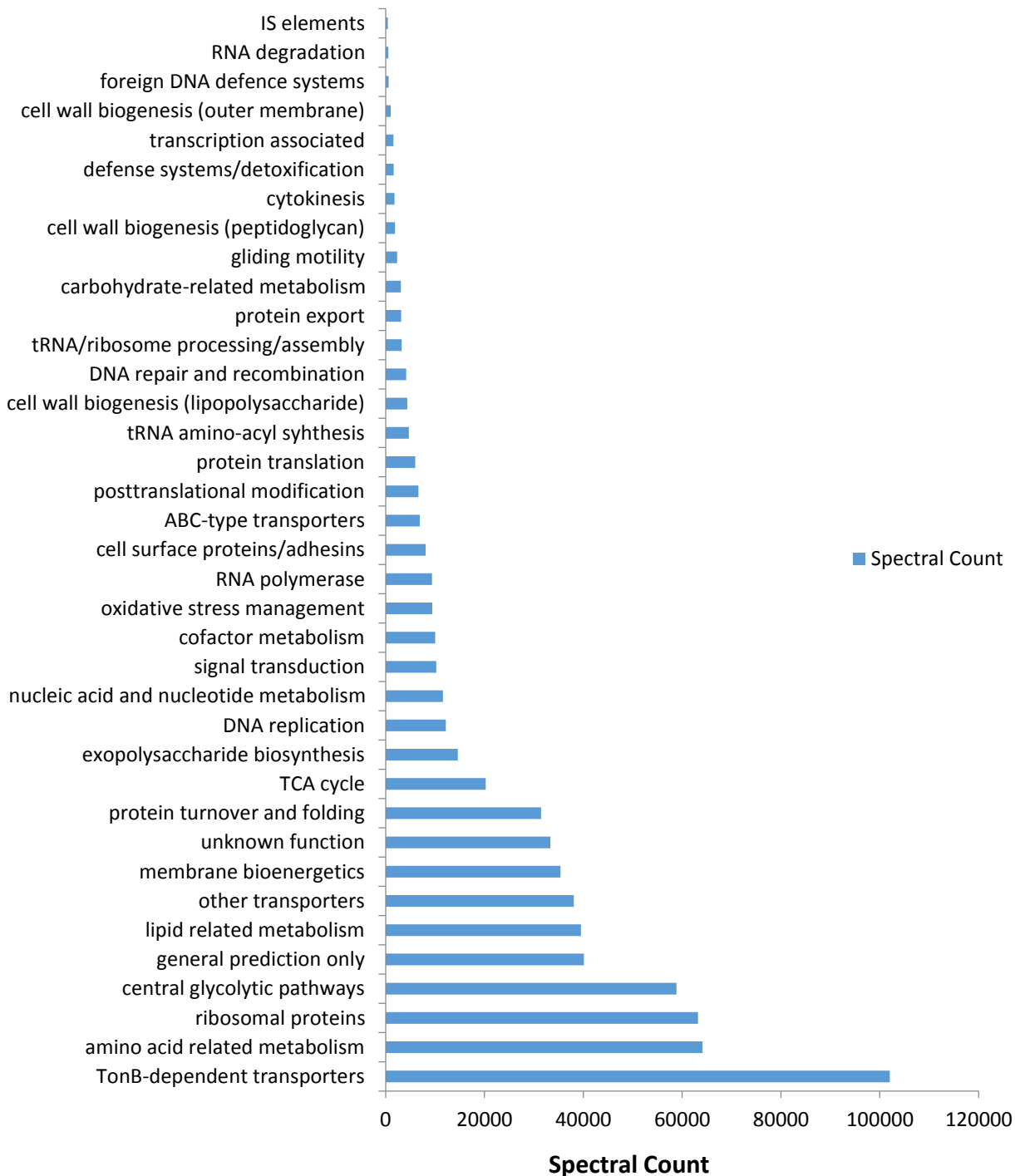


Figure. S3. Spectral abundance (that passed filtration criteria) of *P. torquis* proteins observed in sets organized on the basis of functional class. These spectral counts are summed from all samples.

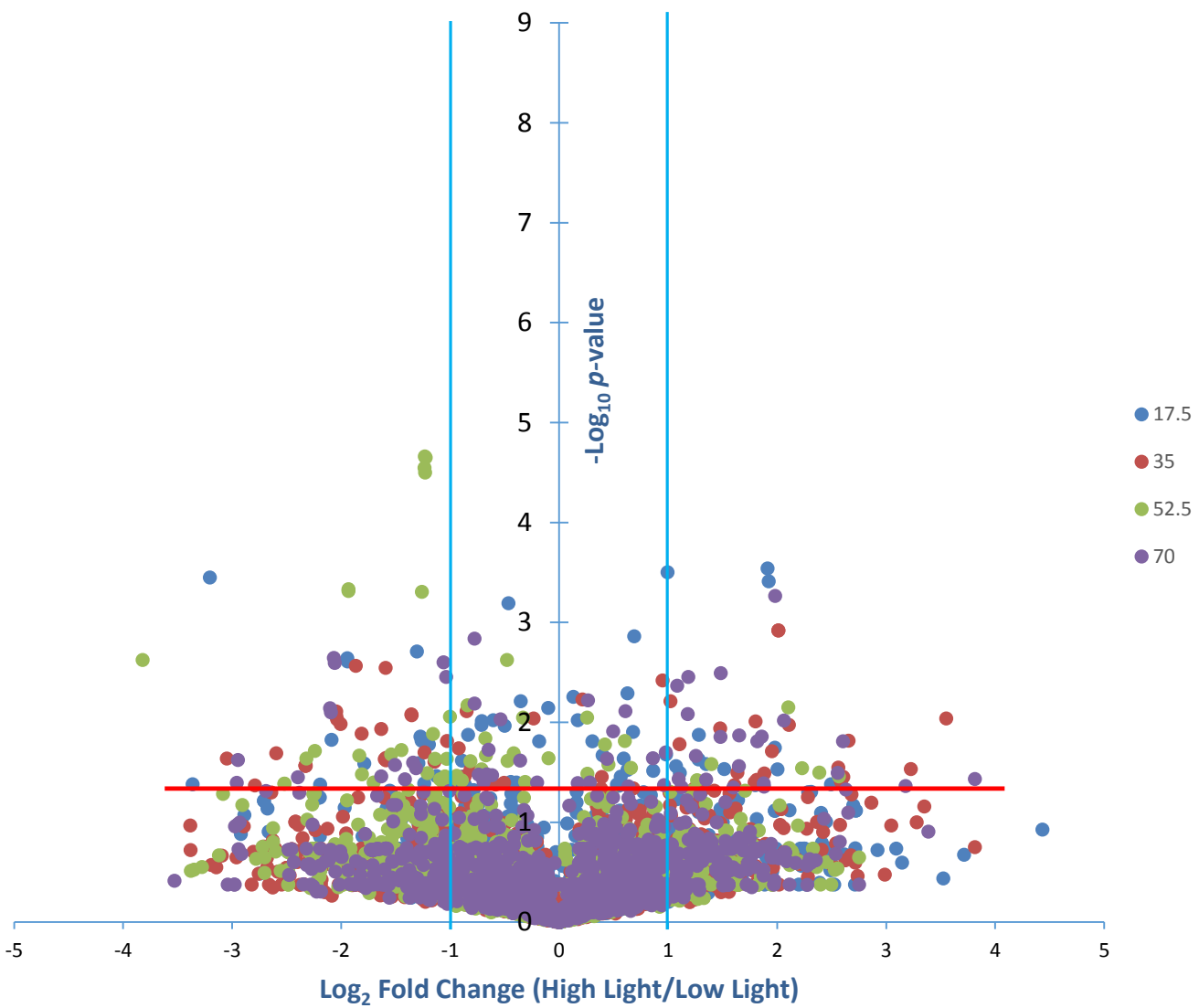


Figure. S4. Volcano plot of 1406 proteins from high light compare to low light., the log ratio of protein fold change were plotted against negative log p value of the beta-binomial distribution analysis from six replicates. Red line represent cutoff for $p\text{-value}=0.05$; blue line represent cutoff for fold change= ± 2 .

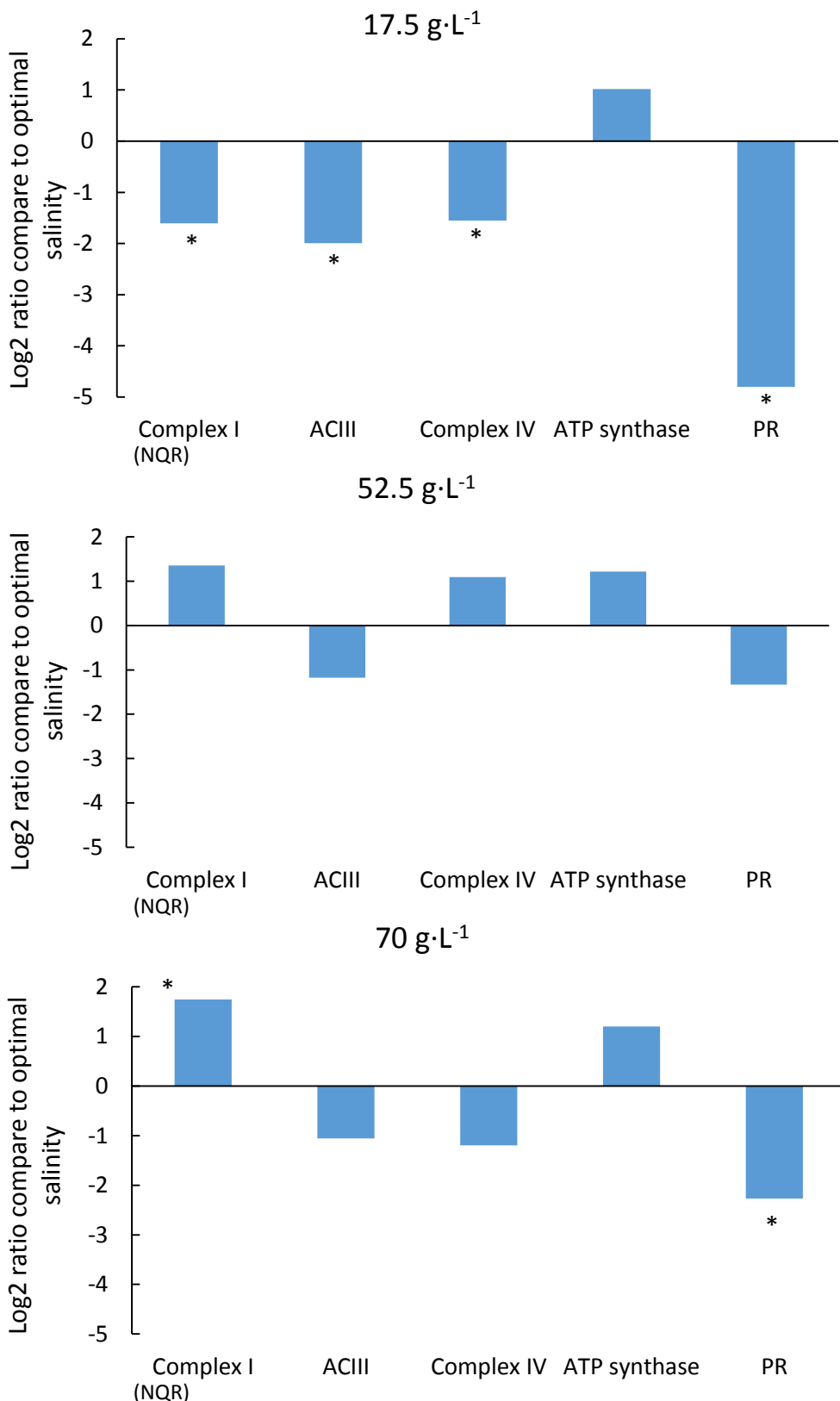


Figure. S5. Proteomic response of electron transport chain proteins under different salinities when compare to optimal salinity condition($35\text{g}\cdot\text{L}^{-1}$). The spectral counts from all three light conditions for each salinity level were pooled together to compare with the optimal salinity ($35\text{g}\cdot\text{L}^{-1}$). Asterisks indicate p value of the fold change is less than 0.05.

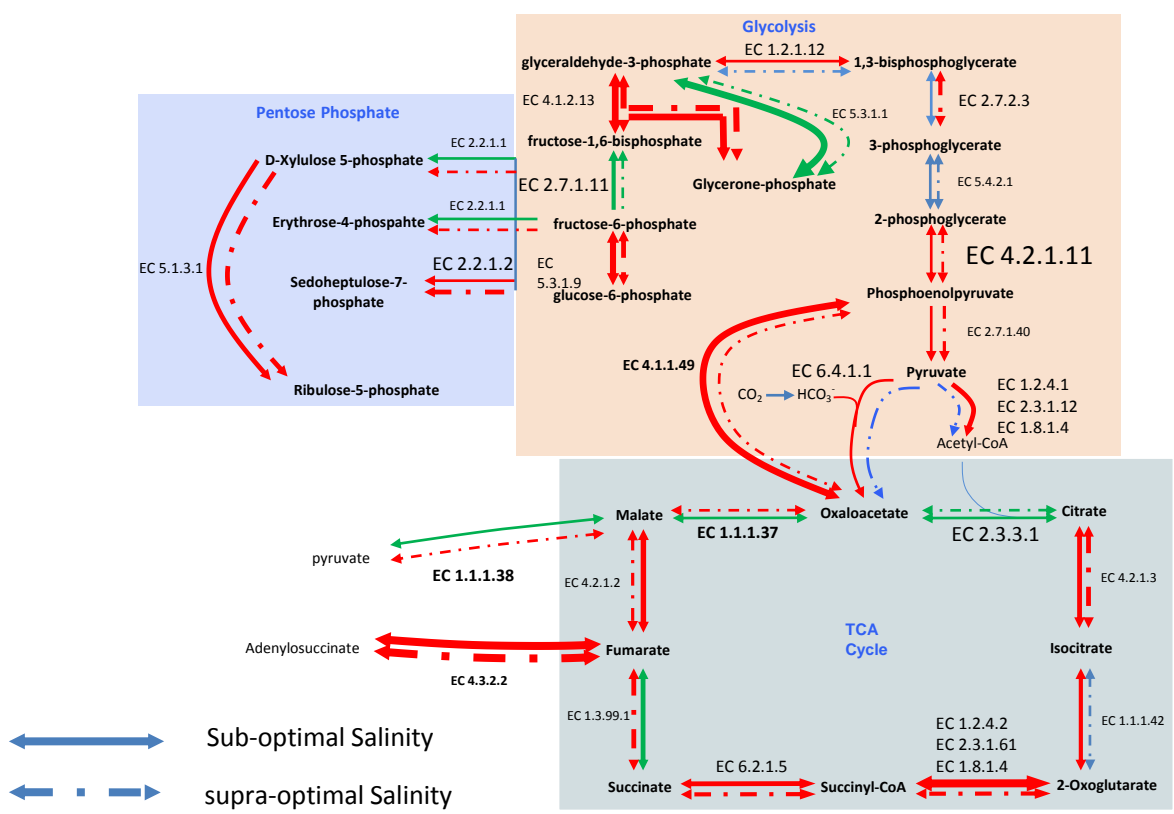


Figure. S6. Diagram of central metabolic pathway change under different salinity. The optimal salinity ($35\text{g}\cdot\text{L}^{-1}$) was used as control to compare with sub- and supra-optimal salinities. Within the metabolic map, red line indicates up-regulation, green line indicates down-regulation, blue line indicates unchanged. The thickness of line imply the degree of change. The size of enzyme code indicates the abundance of the enzyme.

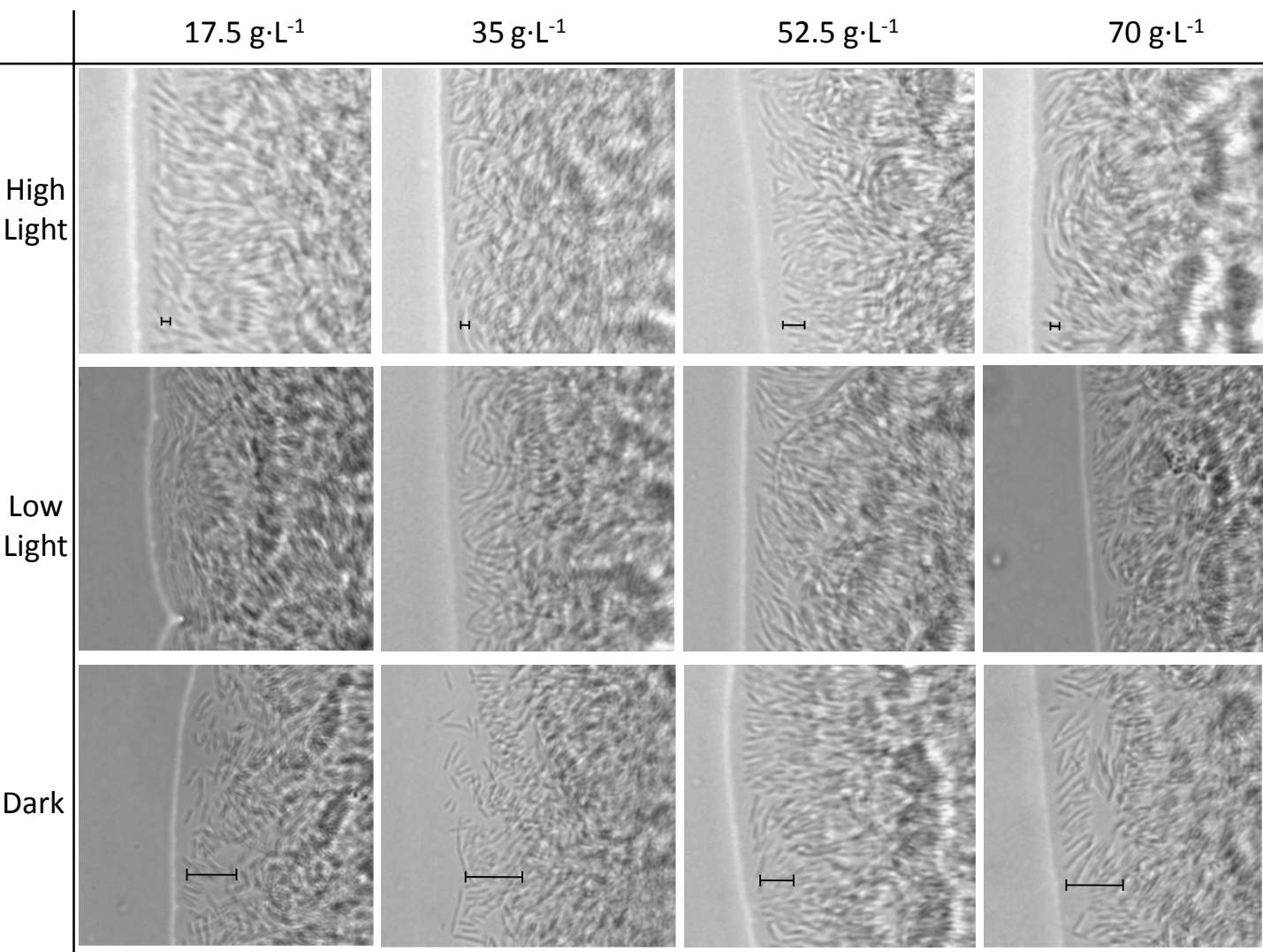


Figure. S7. Gliding motility of *P. torquis* under different salinity and illumination levels. Light intensities were: high light ($20-30 \mu\text{mol photons m}^{-2} \text{ s}^{-1}$); low light ($3-4 \mu\text{mol photons m}^{-2} \text{ s}^{-1}$) and complete darkness ($0 \mu\text{mol photons m}^{-2} \text{ s}^{-1}$). The scale bar indicate the distance from most outside bacteria cell to the main colony which indicate increased gliding motility of *P. torquis* under dark.

Table S1: Spectral count and number of proteins identified by LC-MS/MS from each sample.

Treatment \ Spectra and Protein	Spectral Count	Number of Proteins Identified
17.6 g·L ⁻¹ (High Light) No. A	19039	790
17.6 g·L ⁻¹ (High Light) No. B	19303	758
17.6 g·L ⁻¹ (High Light) No. C	18720	672
17.6 g·L ⁻¹ (Low Light) No. A	18411	804
17.6 g·L ⁻¹ (Low Light) No. B	19787	709
17.6 g·L ⁻¹ (Low Light) No. C	19491	725
17.6 g·L ⁻¹ (Dark) No. A	19160	664
17.6 g·L ⁻¹ (Dark) No. B	18737	793
17.6 g·L ⁻¹ (Dark) No. C	14511	553
35 g·L ⁻¹ (High Light) No. A	14818	581
35 g·L ⁻¹ (High Light) No. B	17104	648
35 g·L ⁻¹ (High Light) No. C	17340	653
35 g·L ⁻¹ (Low Light) No. A	11278	410
35 g·L ⁻¹ (Low Light) No. B	16611	509
35 g·L ⁻¹ (Low Light) No. C	19610	777
35 g·L ⁻¹ (Dark) No. A	17878	570
35 g·L ⁻¹ (Dark) No. B	15033	489
35 g·L ⁻¹ (Dark) No. C	18671	708
52.5 g·L ⁻¹ (High Light) No. A	16165	579
52.5 g·L ⁻¹ (High Light) No. B	13216	424
52.5 g·L ⁻¹ (High Light) No. C	18243	742
52.5 g·L ⁻¹ (Low Light) No. A	12942	574
52.5 g·L ⁻¹ (Low Light) No. B	18139	751
52.5 g·L ⁻¹ (Low Light) No. C	18466	788
52.5 g·L ⁻¹ (Dark) No. A	16658	591
52.5 g·L ⁻¹ (Dark) No. B	12425	427
52.5 g·L ⁻¹ (Dark) No. C	18788	753
70 g·L ⁻¹ (High Light) No. A	15477	676
70 g·L ⁻¹ (High Light) No. B	17805	769
70 g·L ⁻¹ (High Light) No. C	18142	798
70 g·L ⁻¹ (Low Light) No. A	18010	573
70 g·L ⁻¹ (Low Light) No. B	16258	727
70 g·L ⁻¹ (Low Light) No. C	13009	684
70 g·L ⁻¹ (Dark) No. A	17902	578
70 g·L ⁻¹ (Dark) No. B	17046	685
70 g·L ⁻¹ (Dark) No. C	18772	726